Interpretation of VHF radar echoes from a Complex Flow Field

M.L Heron[1], M. O'Shea[2], J. Murphy[2], L. Petersen[3], D. Mollaghan[2] and A. Prytz[1]

[1]Aims@JCU, JCU TropWater, School of Earth and Environmental Sciences, James Cook University, Australia;

[2] Beaufort Research-HMRC,University College Cork, Ireland,

[3] Helzel Messtechnik GmbH, Hamburg, Germany.

mal.heron@ieee.org

Abstract— **Bragg lines on spectra from ocean radar systems are broadened when echoes come into the antenna from different azimuths. Phased-array systems minimise the effects of this by selecting a small target area on the sea surface by beam-forming and range-gating. While phased array systems are better conditioned for high spatial resolution than direction finding systems, in some cases there may be fine structure in the surface current field within the smallest of target areas. In estuaries or other areas where there are sand banks and low islands there is potential for contamination from side-lobes of phased array antennas to contaminate adjacent pixels. This paper uses data from an area of highly complex flow field in Dingle Bay, Ireland to examine the complex structure of Bragg echoes. A numerical hydrodynamic model is used as an aid in understanding the degree of structure to be expected in the Bragg lines, and an improved analysis is described to extract surface current data from the radar echoes.**

Keywords—current monitoring; HF ocean radar; estuaries

I. INTRODUCTION

There is a special challenge for HF ocean radars to map surface currents in coastal areas where there is a high degree of fine structure, mainly due to tides. The phased-array genre of HF ocean radar is the best option for spatial high resolution situations, and the ultimate limitation is often considered to be multiple peaks and broadening of the Bragg lines due to infrastructure in the pixel (Heron, 1985). Often the scale of the structure in the flow field is of the order of the size of the resolution pixels of the radar and there is potential for complexity in the Bragg peaks.

Fig. 1 shows a graph of received power on a range versus Doppler shift set of axes. It is from a WERA phased-array radar with a narrow beam pointing across the central part of Dingle Bay in County Kerry, Ireland. With multiple and broadened echoes like this the conventional analysis often fails to locate the 'correct' peak in the spectrum at a given range. In this paper we will confirm the 1:1 link between Bragg line multifurcation and complexity in the surface current flow coupled with side-lobe contamination.

II. THE SITE

Dingle Bay contains 2 mid-bay barriers, Inch and Rossbeigh peninsulas extending across the Bay divided by a tidal inlet.

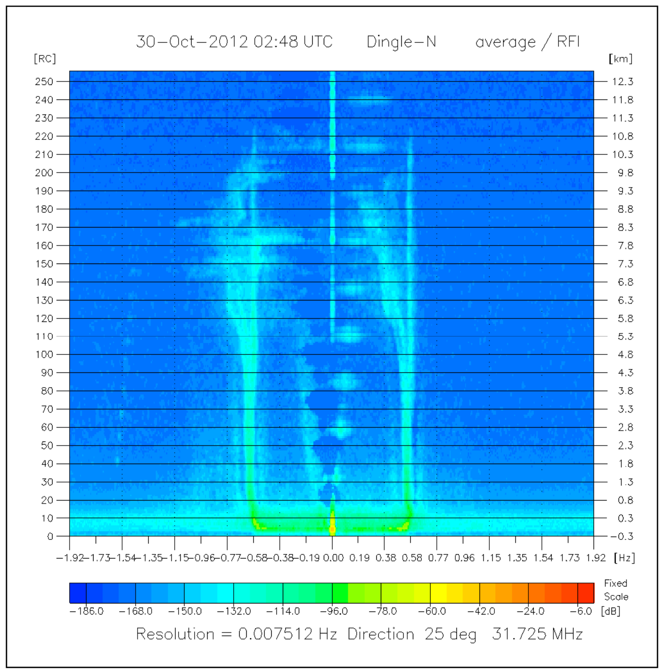

Figure 1. Echo Power contours on range vs Doppler Shift axes. The range is given as the Range-Cell Number (left) and as km (right). The main Bragg echoes are indicated by the approximately parallel bands at about ±0.56 Hz. At a range of about 4 km the Bragg lines bifurcate and at 5km there are clearly 3 separate Bragg 'lines'. The recurring blobs near zero Doppler shift are interference effects.

The Inch peninsula extends from the north to the south across the Bay is located seaward of the Inch peninsula and is over 4 km in length, running from the south shore towards the north. On ebb and flood tides the current in the channel between the barriers can exceed 1 m/s, which produces complexity in the 2D flow field across the Bay. Fig. 2 shows the bathymetry and the layout of the radar system. The sand bars shown here are dynamic and shifting from one storm to the next; it is the understanding of this geomorphology that underlies this project.

III. THE METHODOLOGY

We make two approaches to address this problem. One approach when there is multi-peaking or spectral broadening in the spectrum at one target cell, is to look at adjacent cells to identify trends in the amplitudes of the spectral peaks. The second approach is to examine the effects of side-lobes of the phased-array antenna and to find an analysis solution that will overcome this contamination.

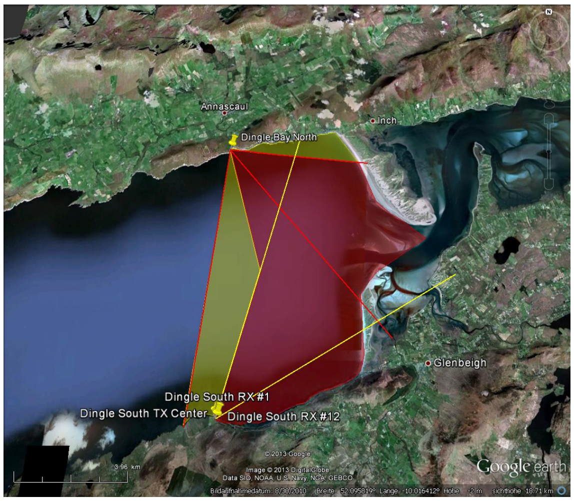

Figure 2. The map of the central part of Dingle Bay showing the 2 barrier headlands and the channel in between. The aerial photo (Google) shows the shallow bathymetry of channels and sandbanks. The geometrical overlays show the configuration of the radar stations. The southern station (St1) scans its beam about the yellow line at 57^{o} E; and the northern station (St2) scans between the red lines. The area common to St1 and St2 is that which may produce current vectors; shown as maroon in the schematic.

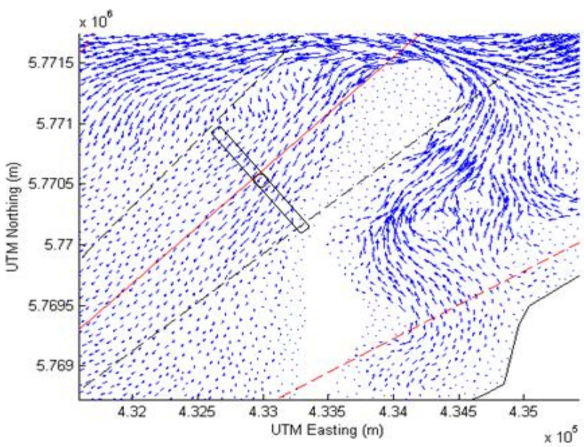

Figure 3. Output from the numerical model with radial lines from Station 1 superposed. The solid red line indicates the centre of the beam and the black dash lines show the angles at which the beam is 3db below the peak. The rectangle shows the 3db contour for the target cell which encompasses both high and low currents. The lower red dash line shows the position of the 1st side-lobe in the antenna pattern.

A. *Spectral Broadening:*

Fig. 3 shows the outline of the 3db echo strength for a target cell superposed on a map of the bathymetry and the currents provided from a Mike DHI model at the time of maximum ebb on 8 November 2012. Fig.4 shows the observed spectrum for the target cell shown in Fig. 3.

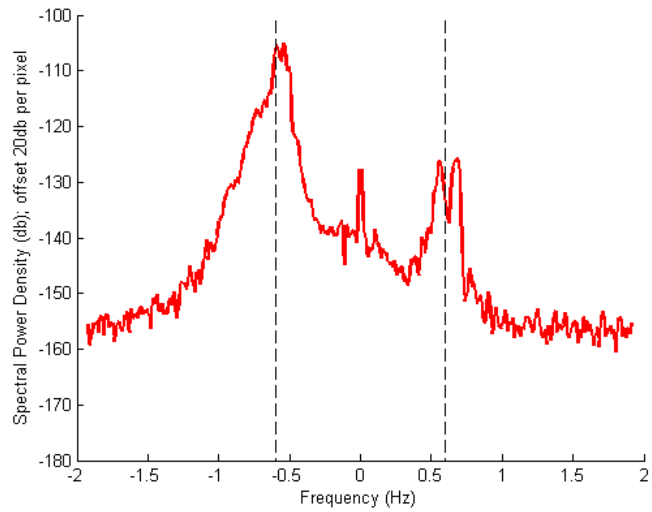

Figure 4. The echo spectrum for the target cell shown in Fig. 3. The vertical dash lines mark the position of the Bragg lines when the radial current is zero. The spectrum has a peak near the zero current line and there is a second peak at a positive offset which indicates a radial component towards the radar station.

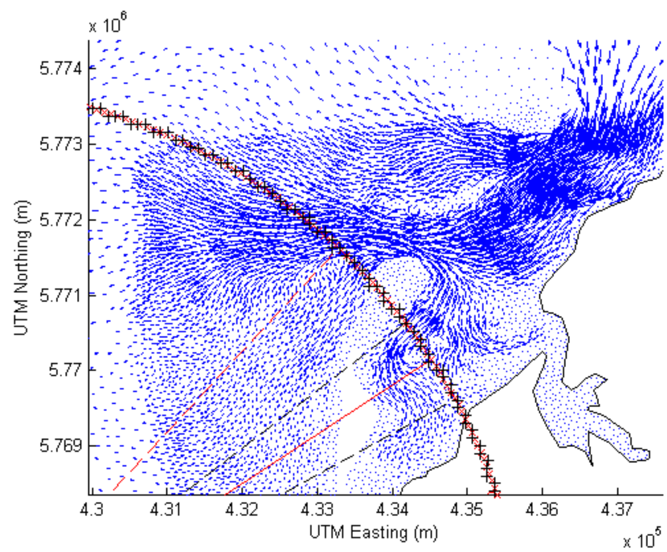

Figure 5. Pixels selected along an arc. The solid red line is the antenna boresight direction, and the black dased lines show the 3 db points on the beam pattern. The red dashed line shows the location of the first side-lobe discussed in the next section (the other side-lobe is off the picture).

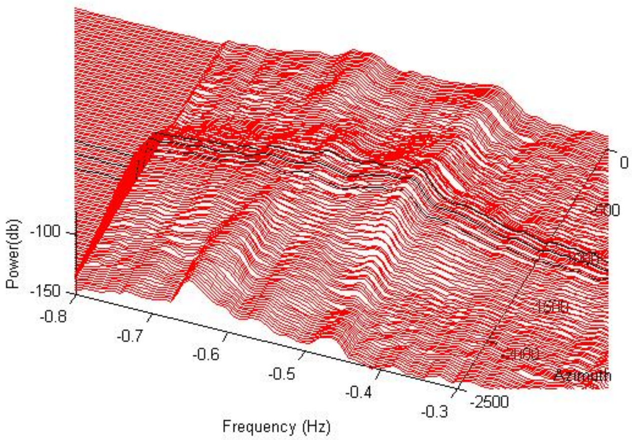

Figure 6. The x and y axes are Doppler shift frequency and azimuth, and the z axis is echo power. The black lines indicate the range annulus corresponding to the arc in Fig. 5. The Doppler frequency of the Bragg peaks is ±0.599 Hz when the surface current is zero.

Consider the grid points (for radar spectra) located on an arc within a narrow band of ranges as shown in Fig.5. It is clear that the spacing of the grid points is less than the resolution of the radar beam, but as the beam 'sweeps' across a change in surface currents, the Bragg peak will have two peaks, the power of which will change as the transect is made. This is illustrated in Fig. 6. The simplest strategy for analysis is to take the highest Bragg peak at each azimuth interval. The transition from one peak to another is captured within about 2 degrees of azimuth when the 3 db points of the beam pattern are 8.7 degrees apart, thus improving the azimuthal resolution.

B. Side-lobe Contamination

The sweep method to improve azimtuthal resolution may be adversely affected by energy from side lobes. Fig. 7 shows the beam pattern for the 12-element phased-array used in Dingle Bay. It has a 3 db beam width of 8.7^o and the first side lobes are at $\pm 13.9^o$ and are about 13.6 db below the peak of the main beam. It is when the echo power from pixels in the main beam fall more than about 13.6 db below the echo power in pixels in the side-lobes that the azimuthal sweep analysis described above will be contaminated.

In an open ocean situation, contamination from side-lobes for the analysis of first-order echoes is not expected. A reasonable assumption for the angular spread of the gravity waves is given by (Longuet-Higgins, 1963; Heron, 1987):

$$S(k,\theta) = A(k)\, Cos^{2s(k)}\left(\theta/_2\right) \qquad (1)$$

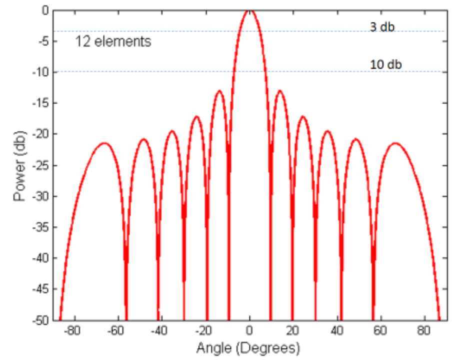

Figure 7. Beam pattern for a 12-element phased array antenna with λ/2 spacing.

where $s(k) \approx 1$ for the Bragg wavelengths of about 8.5 m wavelength. The total energy in the bragg echoes from a given pixel is the sum of the power in the echo from the positively shifted Bragg wave, and that of the negatively shifted Bragg wave. The integrated power in a Doppler shifted spectrum from a pixel at azimuth θ to the direction of the wind is then proportional to

$$P = Cos^2\left(\theta/_2\right) + Cos^2\left((\theta+\pi)/_2\right) \qquad (2)$$

which is identically equal to 1.

It is only when the amplitudes of the Bragg waves change within the scale of the main and side-lobe separation that there is potential for contamination. Fig.8 shows the total spectral power in the Bragg spectra along the transect of arc shown in Fig. 5. The dramatic drop in total power as the beam sweeps to the west of its boresight bearing is due to shallow water and land. In the analysis, the total spectral power is used to detect echoes when the main beam is over land or exposed tidal flats. When the total power falls to less that 10 db below the maximum valee for the transect, the ixel is flagged as unreliable. These pixels may still contain low-power Bragg peaks, but they must be excluded because that vestige of power may be coming from a side-lobe which is still over open water.

IV. RESULTS

Using the azimuthal sweep and the exclusion of pixels with low integrated power it is possible to create a map of radial components of current as shown in Fig. 9. The grid has a characteristic polar appearance because the analysis is done along successive arcs. We chose ranges spaced 200 m apart in order to create a better visual appearnce; there is no reason

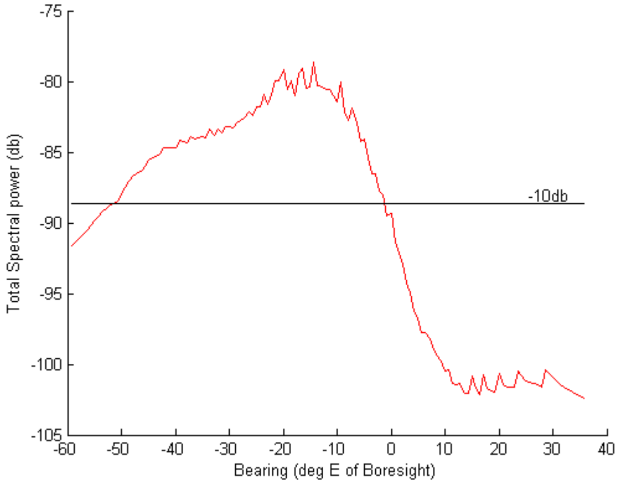

Figure 8. Total power in the Doppler shift spectrum along the transect arc at a range of 8000 m. The drop of over 20 db is due to the main beam covering land or exposed tidal flats.

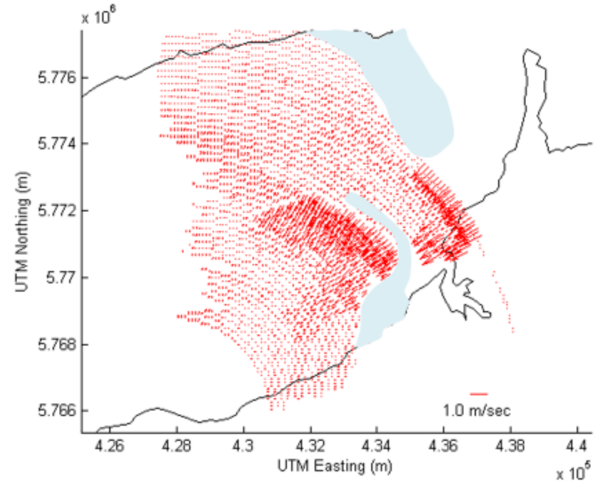

Figure 9. Observed radial surface currents in Dingle Bay at 1500 UT on 8 November 2012 at the maximum tidal ebb. The black line is the hard coast line. The light blue shading is an estimate of the location of the sand bars using the radar data.

why the grid could not be completely filled. The analysis follows the procedures outlined and the resulting plot is not smoothed or averaged. The criteria for excluding pixels are based on the total power in the spectrum compared with that across the transect. For this analysis we set a 10 db level, guided by the side-lobes being theoretically 13.6 db below the main lobe. The result shown in Fig. 9 is that there are some seemingly genuine sea echoes which arise from pixels on land. There appears to be a rotation of a few degrees in the positioning of the grid in the context of the hard coastline plotted in black. The blue shading was drawn onto the Figure to satisfy the surface currents plotted from radar data. This shading represents areas where there may be sand bars or exposed tidal flats. The rotation discrepancy observed between the radar data and the plot of the coastline extends to the positioning of the sand bars on the underlying image in Fig. 2. The reconciliation of these issues is a work in progress because the movement of the sand bars is a key issue to be addressed in the wider project.

V. Conclusion

The complex Doppler shift echo spectra obtained at the Dingle Bay site can be simplified by using the data themselves to flag and exclude pixels in areas that return low echo power. The spatial resolution shown in the map enables us to determine the outline of sand bars and coast lines. The first results for this analysis, shown in Fig. 9 is a remarkable success for the technology of HF ocean radar and its ability to show fine scale structure. In principle, the approach of total power in the Bragg spectra could be mapped to delineate the coastline of a bay or estuary, and this may prove to be a better way to map the coast lines and sand bars.

References

[1] Heron, M.L., Directional spreading of fetch-limited short-wavelength wind waves, J. Phys. Oceanogr., 17, 281-285, 1987.

[2] Heron, M.L., Line Broadening of HF ocean surface radar backscatter spectra, J. Oceanic Eng., OE-10, 397-401, 1985.

[3] Longuet-Higgins, M.S., D.E. Cartwright and N.D. Smith, Observations of the directional spectrum of sea waves using the motion of a flotation buoy, in *Ocean Wave Spectra*, pp 111-136, Prentice-Hall, Englewood Cliffs, N.J., 1963.